

*Letter to the Editor***Age-metallicity relation and chemical evolution of the LMC from UVES spectra of Globular Cluster giants<sup>★</sup>**V. Hill<sup>1</sup>, P. François<sup>1</sup>, M. Spite<sup>2</sup>, F. Primas<sup>1</sup>, and F. Spite<sup>2</sup><sup>1</sup> European Southern Observatory, Karl-Schwarzschild-Strasse 2, 85748 Garching, Germany<sup>2</sup> Observatoire de Paris-Meudon, 92125 Meudon Cedex, France

Received 10 August 2000 / Accepted 13 September 2000

**Abstract.** We report on the first high-resolution spectroscopy of 10 giants in LMC Globular Clusters *in a wide age range*, obtained with the newly commissioned spectrograph UVES at VLT UT2. These observations are used to derive oxygen and iron content of these clusters, and the abundances are then used to cast a more precise view, not only on the age-metallicity relation in the LMC, but also on the chemical evolution of this dwarf irregular galaxy.

**Key words:** stars: binaries: spectroscopic – stars: late-type – Galaxy: globular clusters: individual: NGC 2210, ESO 121-SCO3, NGC 1978, NGC 1866 – galaxies: Magellanic Clouds

**1. Introduction**

The Magellanic Clouds (MCs) possess a large population of stellar clusters of a whole range of ages, including 13 *bona fide* old Globular Clusters in the LMC and only one somewhat younger counterpart in the SMC. The photometry of these clusters has been extensively studied over the years, and especially since HST started producing high quality CMDs reaching the very densest central part of the clusters (Olsen et al. 1998, Johnson et al. 1999).

The opportunities offered by these clusters are twofold: they provide laboratories to study stellar evolution in a range of different conditions (the young and yet metal-poor MC clusters have no Galactic counterparts and serve as a test of stellar evolution models at low metallicities), and give us the opportunity to study the formation and evolution of magellanic-type galaxies (determination of the age-metallicity relation, etc. . .). It is with this second aspect that we will be dealing in this paper.

In particular, the oldest component of these stellar clusters (the *bona fide* old metal-poor globular clusters) can serve as tracers of early epochs of the evolution (halo phases) in several ways: precise determination of ages of these old globular clusters yield estimates of the characteristic time-scales of halo

formation; information on the chemical evolution of the MCs at early stages of their evolution is kept in the atmosphere of the cluster stars; kinematics of the clusters can be used as a tracer of halo structure.

While kinematics issues were addressed at length already some time ago (e.g. Schommer et al. 1992), topics in need of precise metallicities were so far quite tentative: because of the faintness of their members, chemical composition of old and intermediate age clusters were not known with a very good accuracy (low-resolution Ca II IR triplet, photometric estimates). We are now for the first time, thanks to VLT and its efficient spectrograph UVES, in a position to improve dramatically this knowledge with detailed analysis of individual cluster giants fainter than 16 magnitudes.

As part of UVES *Science Verification*, a sample of 10 giants in 4 clusters in a very wide age-range (0.1 to 15 Gyrs) were observed at high spectral resolution ( $R \simeq 40000$ ). In this paper, we present the analysis of this data, derive oxygen and iron content of the four clusters, and use them to further constrain the age-metallicity relation in the LMC. We also present, for the first time, the evolution of the [O/Fe] along time in the LMC, and briefly discuss the implications on the processes driving the chemical evolution of this dwarf irregular galaxy. A future paper (in preparation) will deal with the full analysis of the 20 elements measured in these giants and the full implication on the chemical evolution of the LMC.

**2. Observations**

The observations were performed from the 10 to the 18th of February 2000, as part of the VLT UT2 *Science Verification* of UVES, the UV and Visual Echelle Spectrograph recently commissioned on VLT (D’Odorico et al. 2000). The setting used (RED arm,  $\lambda_{\text{central}} 5800\text{\AA}$ ) provided a wavelength coverage 4800–6800 $\text{\AA}$ . The entrance slit was adjusted to fit the seeing conditions, between 1 and 1.2'', which translate respectively into a resolving power of  $R \sim 45000$  to 38000. The Table 1 gives a short logbook of the observations, together with the achieved S/N (per 0.03 $\text{\AA}$  pixel, at 6000 $\text{\AA}$ ).

Send offprint requests to: V.Hill

<sup>★</sup> based on observations made at the ESO Telescopes in Chile

The spectra were reduced using the UVES context within MIDAS, which performs bias subtraction (object and flat-field), inter-order background subtraction (object and flat-field), optimal extraction of the object (above the sky, rejecting cosmic hits), division by a flat-field frame extracted with the same weighted-profile as the object, wavelength calibration and re-binning to a constant step and merging of all overlapping orders. The spectra were then corrected for barycentric radial velocity and coadded, and finally normalized.

### 3. Abundance analysis

A more detailed discussion will be given in a paper (Hill et al., in preparation) dealing with the full abundance analysis of the 20 elements detected in these giants. We give however here a short summary of the methods used to determine the iron and oxygen abundances.

#### 3.1. Atmospheric parameters

The effective temperature  $T_{\text{eff}}$  and gravity  $\log g$  of each star were determined in a two-step process:

1. The colour and absolute magnitudes of the cluster stars were used to derive the effective temperatures using the Alonso et al. (1999) calibrations for giants, and the gravity using the simple relation between gravity and absolute luminosity (once  $T_{\text{eff}}$  and masses are known). The colour information, together with the derived temperatures and gravities of each program star are given in the Table 2 (columns 1 to 7). For each cluster, the table also lists the reddening, distance modulus, metallicity and masses (isochrones Bertelli et al. 1994) adopted for the computation of the  $T_{\text{eff}}$  and  $\log g$ .
2. In a second step, we used spectroscopic indices to further constrain the atmospheric parameters:
  - $T_{\text{eff}}$  was constrained requiring the excitation equilibrium of Fe I to be fulfilled.
  - $\log g$  was determined from the ionization balance of Fe I and II (and Ti when available)
  - the microturbulence velocity ( $v_t$ ) was determined asking the Fe I abundance to be independent of the line strength.

The temperatures and gravities deduced in that way (columns 8-10 of Table 2) were very close to the ones derived from photometry and were adopted for the rest of the analysis. The only counter-example is NGC1978 LE9, for which the ionization balance requires a gravity 0.5 dex *lower* than predicted. This behaviour is well known in very cool galactic metal-poor giants (field and Globular Clusters), where it is interpreted as a signature of NLTE effects.

The associated uncertainties are expected to be of the order of  $\Delta T_{\text{eff}} = \pm 150\text{K}$   $\Delta \log g = \pm 0.2$   $\Delta v_t = \pm 0.2\text{km s}^{-1}$ . Also listed in Table 2 are the measured heliocentric radial velocity for each star.

**Table 1.** Log book of the observations

Star	MJD	slit "	Exp. h.m	S/N
NGC 1866 B444	51584.10565	1.2	1h30	75
NGC 1866 B1653	51586.04048	1.2	1h00	85
NGC 1866 B867	51591.03805	1.0	1h00	
	51591.08042	1.0	1h00	40
NGC 1978 LE8	51590.03804	1.2	1h15	
	51590.09094	1.2	1h15	70
NGC 1978 LE9	51589.03189	1.0	1h15	
	51589.08487	1.0	1h15	70
ESO 121-SC03 M313	51585.04156	1.0	1h30	
	51585.10510	1.0	1h30	45
ESO 121-SC03 M167	51587.03766	1.0	1h15	
	51588.10597	1.0	1h15	60
NGC 2210 B4364*	51586.08746	1.0	1h40	55
NGC 2210 B110*	51586.08746	1.0	1h40	30
NGC 2210 B4793	51588.04009	1.0	1h30	60

Identifications for the clusters: NGC 1866: Brocato et al. 1989; NGC 1978: Lloyd Evans 1980; ESO 121-SC03 Mateo et al 1986; NGC 2210 Brocato et al. 1996.

\* the two stars were observed on the same slit (12 arcsec long).

#### 3.2. Abundance determinations

The abundance calculations were made using model atmospheres from the MARCS suite: the models of Plez (1998, a grid especially computed for cool giants in the metallicity range  $[\text{Fe}/\text{H}] = -1$  to  $+0.3$  dex) were used for the three more metal rich clusters, and Gustafsson (1975), for the more metal poor cluster NGC 2210.

The abundance of iron was determined using the equivalent width of up to 70 lines of Fe I and up to 10 Fe II lines. Aluminium lines (Al I 6696.03Å and 6698.67Å) were also measured to check for possible deep-mixing effects (cf. Sect. 4.2). Oxygen abundances, on the other hand, were determined from the forbidden [OI] 6300Å line, by comparing the line directly to synthetic spectra. The molecular dissociative equilibrium was taken into account while computing the synthesis, including CO, CN, C<sub>2</sub>, and TiO molecules. For the two younger clusters (NGC 1866 and NGC 1978), a telluric line was contaminating the [OI] 6300Å line, and was removed using the spectra of extremely metal-poor turnoff stars observed during the same nights. Examples of the [OI] fits are displayed in Fig. 1, and the measured abundances obtained for Fe, O and Al are displayed in Table 2 col. 12-14.

## 4. Results

### 4.1. Cluster metallicities

Both ESO 121-SC03 and NGC 1866 are found to have metallicities similar to what was previously assumed in the literature. ESO 121-SC03 has a mean iron abundance  $[\text{Fe}/\text{H}] = -0.91 \pm 0.16$  (2 stars) compared to  $-0.93 \pm 0.2$  in O91 (Ca IR triplet) and  $-0.9$  in Mateo et al. (1986, BV photometry), while NGC 1866

**Table 2.** Photometry, atmospheric parameters and measured abundances for the program stars.

NGC 1866 $E(B - V)=0.06$ ( $M - m$ )=18.6 [Fe/H]=-0.4 Mass=5(4) $M_{\odot}$													
Star	$V$	$(B - V)$		Ref.	$T_{\text{eff phot}}$	$\log g_{\text{phot}}$	$T_{\text{eff}}$	$\log g$	$v_t$	$V_{\text{helio}}$	[Fe/H]	[O/Fe]	[Al/Fe]
B444	15.49	1.51		1	4021	1.0	4020	1.0	1.9	300.5	-0.45	0.03	-0.23
B1653	15.01	1.49		1	4048	0.8	4050	0.8	2.0	300.7	-0.48	0.06	-0.27
B867	16.60	1.14		1	4550	1.7	4550	1.9	1.8	298.2	-0.56	0.14	-0.25
NGC 1978 $E(B - V)=0.08$ ( $M - m$ )=18.5 [Fe/H]=-0.4 Mass=2.0 $M_{\odot}$													
Star	$V$	$(B - V)$	$(J - K)$	Ref.	$T_{\text{eff phot}}$	$\log g_{\text{phot}}$	$T_{\text{eff}}$	$\log g$	$v_t$	$V_{\text{helio}}$	[Fe/H]	[O/Fe]	[Al/Fe]
LE8	16.71	1.66	1.09	2,3	3860/4000	0.8	3860	0.7	1.9	292.2	-1.10	0.45	0.28
LE9	16.85	1.77	0.94	2,3	3734/3800	0.8	3750	0.3	1.9	294.7	-0.82	0.30	-0.07
ESO 121-SC03 $E(B - V)=0.03$ ( $M - m$ )=18.5 [Fe/H]=-1 Mass=1.0 $M_{\odot}$													
Star	$V$	$(B - V)$		Ref.	$T_{\text{eff phot}}$	$\log g_{\text{phot}}$	$T_{\text{eff}}$	$\log g$	$v_t$	$V_{\text{helio}}$	[Fe/H]	[O/Fe]	[Al/Fe]
M313	17.05	1.29		4	4224	1.1	4220	1.1	1.7	310.5	-0.89	0.15	-0.43
M167	16.74	1.47		4	3999	0.9	4000	0.9	1.7	313.9	-0.93	0.15	-0.33
NGC 2210 $E(B - V)=0.06$ ( $M - m$ )=18.4 [Fe/H]=-2.0 Mass=1.0 $M_{\odot}$													
Star	$V$		$(V - I)$	Ref.	$T_{\text{eff phot}}$	$\log g_{\text{phot}}$	$T_{\text{eff}}$	$\log g$	$v_t$	$V_{\text{helio}}$	[Fe/H]	[O/Fe]	[Al/Fe]
B4364	16.22		1.39	5	4261	0.7	4260	0.7	1.8	342.2	-1.78	0.02	0.47
B110	16.89		1.21	5	4570	1.2	4570	1.0	1.8	344.2	-1.81	0.21	-0.14
B4793	16.12		1.41	5	4231	0.6	4230	0.7	1.8	338.8	-1.68	0.19	0.00

References: 1: Brocato et al. 1989 2: Will et al. 1995 3: Ferraro et al 1995 4: Mateo et al. 1986 5: Brocato et al. 1996

Note: The measured  $(V - I)_{\text{Cousins}}$  were converted into  $(V - I)_{\text{Johnson}}$  (suited for the Alonso et al. (1999) temperature calibration) using the relation  $(V - I)_{\text{Johnson}} = 1.273 \times (V - I)_{\text{Cousins}} - 0.05$ .

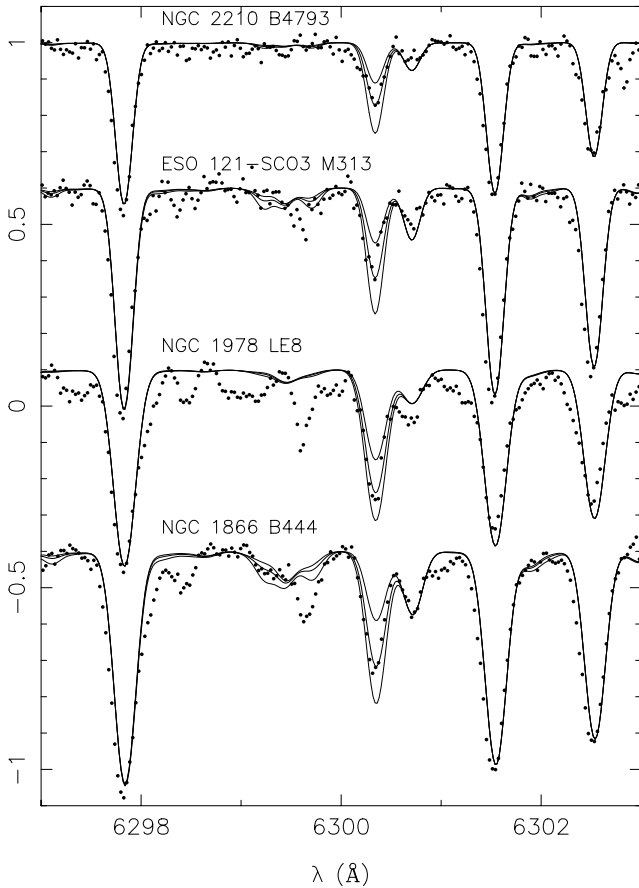


**Fig. 1.** Examples of oxygen line synthesis. Three synthesis are shown in each case, computed with the best fitting [O/H] value and  $\pm 0.2$  dex. The spectra were shifted vertically for lisibility purposes.

has a mean iron abundance  $[\text{Fe}/\text{H}] = -0.50 \pm 0.1$  (3 stars), in very good agreement with Hilker et al. (1995) who derived  $[\text{Fe}/\text{H}] = -0.46$  using Strömgen photometry (there are no previous spectroscopic determinations of metallicity of NGC 1866).

On the other hand, two clusters are found to have a metal-content significantly different from the previously assumed values:

**NGC 2210:** The mean iron abundance of the 3 giants in this cluster is  $[\text{Fe}/\text{H}] = -1.75 \pm 0.1$ , whereas Olszewski et al. (1991; hereafter O91) derived  $-1.97 \pm 0.2$  from 4 similar giants. These two values taken at face are only marginally consistent, but taking into account that the O91 metallicity indicator are calcium lines calibrated to  $[\text{Fe}/\text{H}]$  using galactic globular clusters as comparison, this difference might even vanish completely. In effect, as it is discussed in Sect. 6 and appears clearly in Table 2, the [O/Fe] ratio in NGC 2210 is lower than in galactic globular clusters of the same metallicity. In fact, as will be developed in the main paper of this series (in preparation), all  $\alpha$ -elements, including calcium, are also less abundant than in the galactic clusters. Hence using the Ca II IR triplet would lead to systematically low  $[\text{Fe}/\text{H}]$  estimates, by  $\sim 0.2$  dex.

**NGC 1978:** The mean iron abundance derived from the 2 giants in NGC 1978 is  $[\text{Fe}/\text{H}] = -0.96 \pm 0.2$ , whereas O91 derived  $-0.42 \pm 0.2$  from the two *same* stars. It has to be emphasized that these stars are the coolest giants of our sample, and the analysis of such objects is always difficult, due to the presence of molecular features, and to the more uncertain stellar parameter determination ( $T_{\text{eff}}$  and gravity). However, a very simple test can be performed: in Fig. 2, we overplotted Fe I lines of NGC 1978 LE8 and LE9 to those of NGC 1866 B1653. B1653 is at least 200 K hotter than the NGC 1978 giants, since it does

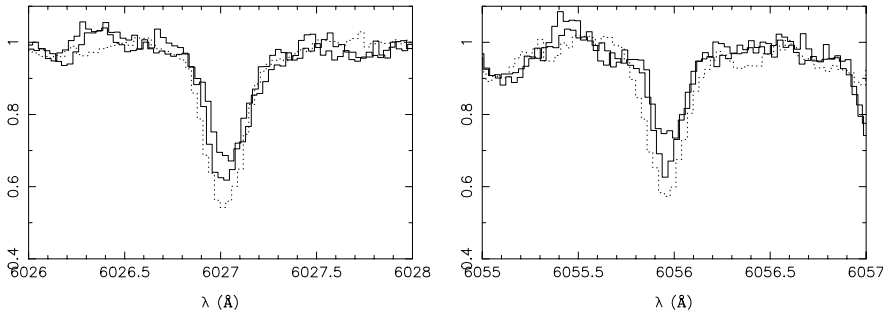


**Fig. 2.** Fe I lines of NGC 1978 LE8 and LE9 (upper and lower solid lines) compared to the 200-300 K hotter star NGC 1866 1653 (dotted line).

not show any TiO bands, whereas LE8 and LE9 do (dissociation of TiO is too efficient for  $T_{\text{eff}}$  hotter than 3900-4000K), and however, the Fe I lines of B1653 are larger than the ones of LE8 or LE9. NGC 1978 therefore *has to be* significantly more metal poor than  $-0.5$  dex.

Another interesting issue is that NGC 1978 has a high ellipticity and a broadened red giant branch and clump, that could be due to the merging of two individual clusters. Alcaino et al. (1999) proposes that the two clusters should have similar ages (explaining the sharp turnoff region), but different metallicities (differing by  $\sim 0.2$  dex) depending on the location in the cluster. The two giants studied here are indeed located in the south-east of the cluster, where the most metal-poor population is expected. It would be extremely interesting to study systematically the abundances of individual stars as a function of location in the cluster and in the CMD.

#### 4.2. Oxygen abundance and deep mixing effects

Oxygen abundances in evolved red giant stars, can be affected by internal mixing phenomena bringing internally-processed material to the surface of the star. The oxygen abundance observed at the surface of the star in this case is not the same as the one the star was born with. Before using  $[\text{O}/\text{Fe}]$  ratios for chemical evolution purposes, we therefore checked the status of mixing in our stars.

In the CNO cycle of hydrogen burning, the final oxygen abundance is very little affected, the cycle basically turning C into N. So that giants experiencing “normal” shallow mixing do not show depleted nor enhanced oxygen. However, other cycles involving oxygen, such as the Ne-Na and the Mg-Al cycles may occur at hotter temperature and hence deeper inside the star. If mixing mechanisms reach deep enough within the star, the products of such cycles can be brought up to the surface, where depleted O and Mg, and enhanced Na and Al can be observed. A very good tracer of deep mixing are the anti-correlations O-Na, Mg-Al, or the even more spectacular O-Al. In our Galaxy, giants in globular clusters and similar giants in the field do not behave similarly: while O-Na O-Al anti-correlations are commonly observed in globular clusters of various metallicities (e.g. Shetrone 1996, Kraft et al. 1998), field stars of comparable evolutionary stage and metallicities show no such trends. This difference is generally attributed to environment effects within the clusters.

In Fig. 3, we have plotted the data points of the 5 giants in the 2 older LMC clusters (ESO 121-SC03 and NGC 2210)

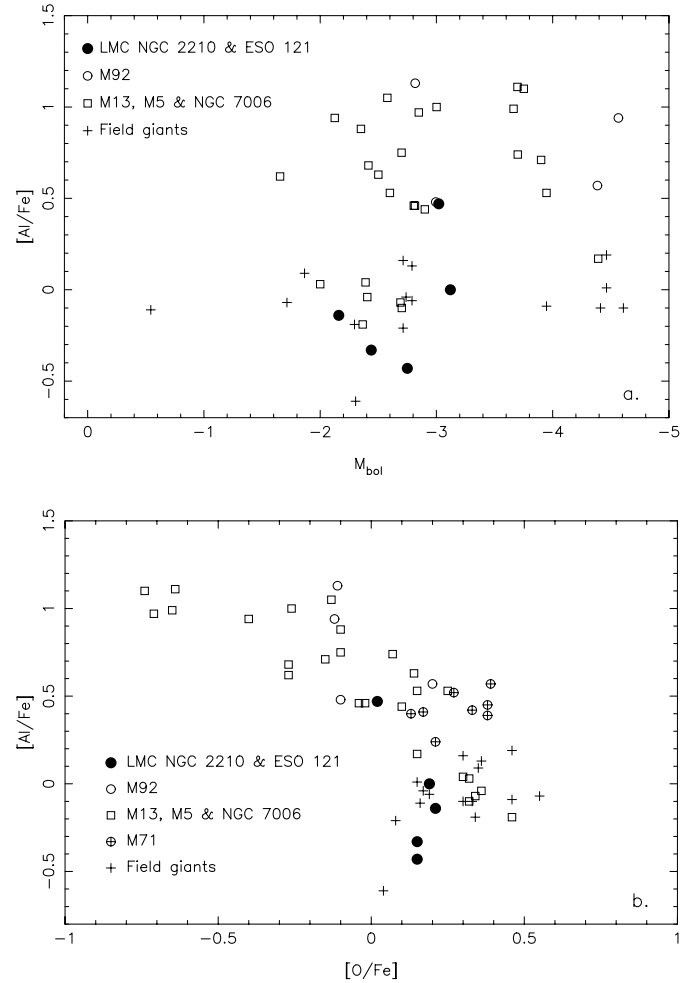


**Fig. 3a and b.**  $[\text{Al}/\text{Fe}]$  abundances for the stars in NGC 2210 and ESO 121-SC03 are plotted, against bolometric magnitude in panel a., and as a function of  $[\text{O}/\text{Fe}]$  in panel b. Overimposed are various samples of red giants in Globular clusters and in the field of our Galaxy (see text for references), illustrating the difference of mixing experienced by field and cluster stars. With one exception (NGC2210 B4364), the LMC old cluster giants clearly follow the galactic field behaviour.

together with data for classical galactic globular clusters of three different metallicities covering the same metallicity range as the LMC clusters. M92 has  $[\text{Fe}/\text{H}] = -2.2$ , M13, M5 and NGC7006 have  $[\text{Fe}/\text{H}]$  from  $-1.$  to  $-1.5$ , and M71 is more metal-rich with  $[\text{Fe}/\text{H}] = -0.8$ . All data (galactic clusters and field) are from

Shetrone (1996), except NGC7006 which is from Kraft et al. (1998). The upper panel shows how the Al overabundances are linked to the evolutionary stage of the giants (where  $M_{\text{bol}}$  traces evolution), and in the lower panel is displayed the O-Al anti-correlation. Also displayed are the galactic field giants, which clearly do not follow the same trend, although spanning the same  $M_{\text{bol}}$  range.

Out of our five LMC old cluster giants, however, only one (NGC 2210 B4364) has a high [Al/Fe] ratio, while the four others have [Al/Fe] ratios similar or even slightly lower than those of the field giants of comparable bolometric magnitudes, suggesting that these four giants *have not experienced major deep mixing events*. The anti-correlation between [Al/Fe] and [O/Fe] is also not observed as such (the LMC sample is far too small), but as expected, the star which is Al-rich is also O-poor: B4364 has most probably dredged up material processed through Ne-Na and Mg-Al cycles.

From panel b. of Fig. 3, it is striking that not only are the [Al/Fe] ratios low compared to galactic globular cluster stars, but that the LMC globular cluster giants seem to define a lower-envelope to the anti-correlation: [O/Fe] seems to be systematically lower in the LMC giants. Galactic cluster giants which have [Al/Fe] close to zero (where the deep mixing mechanism is not acting), have [O/Fe] values of the order of +0.4 dex, whereas our four LMC giants with low Al have [O/Fe]=+0.15 to +0.20 dex. If confirmed on larger samples, this [O/Fe] difference between LMC and Galactic clusters could be attributed to a difference in the chemical evolution of the two galaxies.

## 5. Evolution of metallicity with age in the LMC

### 5.1. New estimations of cluster ages

Many papers have recently discussed the ages of the old Magellanic clusters compared to their Galactic counterparts (Johnson et al. 1999, Olsen et al. 1998, Brocato et al. 1996), coming to the common conclusion that Galactic and Magellanic clusters could have been drawn from the same parent population. However, all age determination methods are dependent (through direct or less direct ways) on the assumed chemical composition of the clusters (overall metallicities but also  $\alpha$ -element abundances). We are now for the first time, in a position to improve dramatically this knowledge with precise abundances of individual cluster giants.

ESO 121-SCO3 and NGC 1866 were found to have the same metallicity as previous estimations and, as a consequence, no effect on the age of these clusters is expected.

For NGC 2210, on the other hand, our [Fe/H] determination is +0.25 dex higher than the value generally assumed to determine the age of the cluster. Age determination by isochrone turnoff fitting is sensitive to the adopted metallicity, an increase of 0.25 dex inducing up to 2 Gyrs younger ages (cf Fig. 10 of Johnson et al. 1999). But we found on the other hand, that NGC 2210 is oxygen poor compared to similar Galactic clusters, by  $\sim -0.2$  dex. In this case, the opposite effect on the isochrones locus of a higher iron and lower  $\alpha$ -element content

cancels out almost exactly, so that the age of NGC 2210 should remain very similar to the age of the old Galactic clusters.

NGC 1978 was found 0.54 dex more metal deficient than previous estimations, but the stars we have studied are rather cool and this result is more uncertain. If this metallicity is confirmed, the effect on age would be of a few tenths of billion years, making the cluster  $\sim 10$ -20% older than its current 2.2 Gyrs estimate.

### 5.2. Age-metallicity relation

The LMC cluster distribution has a long-known peculiarity: both metallicity and age distributions are bimodal, with a well defined *gap* between 3-4 Gyrs and 10-12 Gyrs, corresponding to a minimum of the metallicity distribution between  $\sim -1.0$  and  $\sim -1.5$  dex. This bimodality has been interpreted as the signature of two bursts of star formation, an early one giving birth to the 12-15 Gyrs clusters and a more recent one some 3 Gyrs ago, possibly triggered by tidal interaction of the LMC with our Milky Way. Although the validity of such a conclusion on the global history of the LMC is still a matter of debate (is the cluster formation directly linked to the global star formation? what is the current rate of cluster disruption in the LMC and what was it in the past?), it is of great interest to investigate whether hints of this bimodal star formation can also be found in the age-metallicity relation. Both clusters (see for example Geisler et al. 1997 and Olszewski et al. 1991) and planetary nebulae (Dopita et al. 1997) have been used for this purpose, clusters having more precise age determinations, while planetary nebulae have more accurate chemical composition determinations (O, Ne, Ar, S).

In Fig. 4, the newly derived abundances of the four clusters studied here are overplotted onto the cluster sample of Geisler et al. (1997) (panel a., metallicity is traced by [Fe/H]) and the planetary nebulae (PN) sample of Dopita et al. (1997) (panel b. where metallicity is traced by [ $\alpha$ /H]). The ages of the old ( $>10$  Gyrs) clusters were not taken from Geisler et al. 1997, but adopted from more precise determinations using deep CMDs (Brocato et al. 1996, Olsen et al. 1998 and Johnson et al. 1999) and brought to the same scale using an age of 14 Gyrs for the Galactic comparison clusters. Overplotted are predictions from Pagel & Tautvaišienė (1998) semi-empirical model for two different star formation regimes: the full line is a continuous star formation rate, whereas the dashed line arise from two strong star formation episodes (14 and 3 Gyrs ago respectively) separated by a low star formation period. In panel b., the abundances plotted are, in the case of PN, a mean of Ne, S and Ar, and for the four program clusters, the O abundance. In both cases, as first claimed by Dopita et al. (1997), the age-metallicity distribution seems to be compatible with a burst of star formation some 3 Gyrs ago, triggering an increase of metal-abundances by a factor  $\sim 3$  around this age. Of course, our sample is too small to be conclusive by itself, but the confirmation that there indeed exist clusters (NGC 1978) as young as 2 Gyrs and as metal-poor as clusters of ages 9-10 Gyrs (ESO 121-SCO3) is by itself an interesting conclusion.

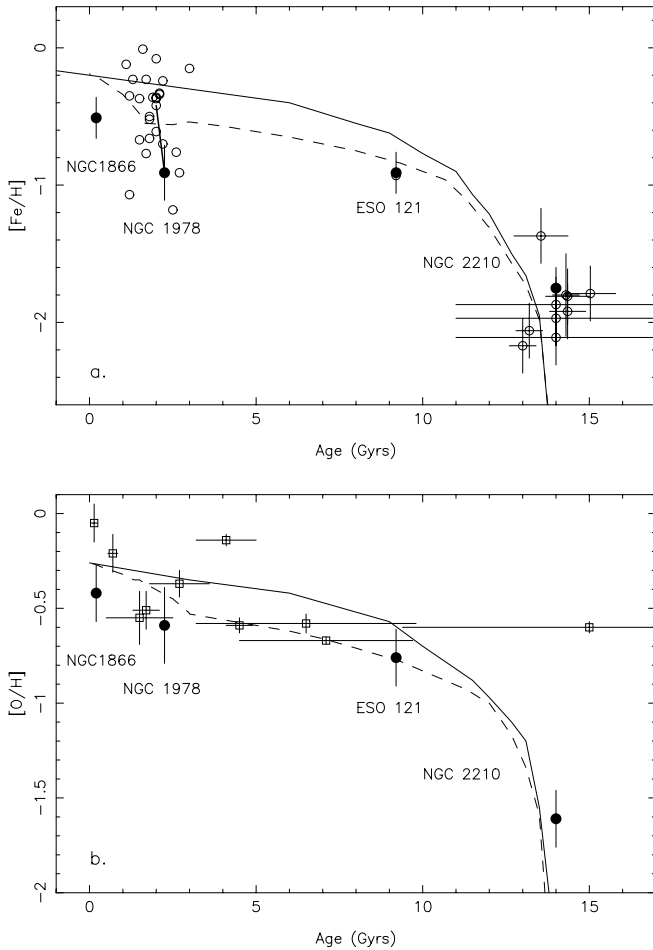


**Fig. 4a** – Age-metallicity relation derived from the four clusters in this paper, together with the data for LMC clusters from Geisler et al. (1997). Overplotted is a theoretical age-metallicity relation from a model using a continuous (thin line) and a bursting (dashed line) SFR (Pagel & Tautvaišiene 1998). The same clusters from the two sources are joined by thick lines. **b** – Age-abundance for oxygen in the LMC, from the four clusters in this paper, together with data for PN from Dopita et al. (1997). Curves as in a-.

## 6. Oxygen over iron ratios and chemical evolution

The most powerful tool available to study the chemical evolution of a galaxy is to follow the behaviour, along time, of the abundance of elements which trace various nucleosynthetic channels and sites. In particular, the evolution of elements produced in different mass-range progenitor stars, gives insight on the IMF and the SFR of the parent galaxy. The most well known such ratio is the  $[O/Fe]$ , which evolution along time (or metallicity) allows to constrain the ratio of the number of massive supernovae (SNII) over supernovae type Ia (SNIa). Up to recently the detailed study of the chemical composition of Magellanic objects were mainly restricted to the brightest stars, namely the young supergiants (cf e.g. Luck et al. 1998, Hill et al. 1995) and to the H II regions, which trace matter younger than  $\approx 0.1$  Gyr. We are now in the position to *follow along time*, the evolution of element ratios.

In the hypothesis that oxygen has not been depleted in the four old LMC cluster giants (all except NGC2210 B4364, see Sect. 4.2), we can now understand the chemical evolution implications of the observed  $[O/Fe]$  ratios.

Fig. 5 displays the observed  $[O/Fe]$  versus  $[Fe/H]$  locus of our LMC sample, compared with the predictions of two families of models computed for the LMC (see caption for details). On the left panel is the semi-empirical model by Pagel & Tautvaišiene (1998), which use the same IMF and yields than in the solar neighbourhood (SN), a star formation rate (SFR) proportional to gas content, a gradual inflow of unprocessed material and galactic wind proportional to the SFR. Their prescriptions include a  $[O/Fe]$  ratio at present time such that  $[O/Fe]_{LMC}=[O/Fe]_{SN}$  at present time. Two models are considered: one where the SFR is continuous, and the other where two bursts occur 14 Gyrs and 3 Gyrs ago respectively. On the other hand, on the right panel of Fig. 5 are models by Tsujimoto et al. (1995) which, at variance with the Pagel & Tautvaišiene (1998), allow the IMF slope to change such that the  $[O/Fe]_{LMC}=-0.2$  at present time.<sup>1</sup> The IMF needed to fulfill this constraint (where  $[O/Fe]_{LMC} \neq [O/Fe]_{SN}$ ) is steeper in the LMC than in the SN (in both continuous and bursting SFR models).

Interestingly, none of the two families of models appear to be able to reproduce the observed  $[O/Fe]$  of LMC clusters: while Tsujimoto et al. (1995) can almost reproduce the low  $[O/Fe]$  of the metal-poor cluster (thanks to their steeper IMF), they cannot reproduce the relatively high  $[O/Fe]$  of the younger clusters at all; Pagel & Tautvaišiene (1998) on the other hand, predict compatible  $[O/Fe]$  in the young population, but too high  $[O/Fe]$  for the older clusters.

The main lesson which can be learned from Fig. 5 is that, if the low  $[O/Fe]$  ratio in the older LMC clusters is confirmed, then the  $[O/Fe]$  run with increasing metallicity would be extremely flat. This is a hint that the LMC chemical evolution might have been driven by a different fraction of SN II/SN I than in our own galaxy, SN I contributing a larger fraction of the iron in the LMC than in the solar neighbourhood. This finding is still speculative at this point, as we definitely need larger samples, both of globular cluster and old field giants in the LMC to demonstrate it. Also, extending this work to the SMC would be a complementary approach to understand the role of the parent galaxy morphology on chemical evolution.

*Acknowledgements.* We thank the Science Operations on Paranal and the UVES Science Verification team for the conduction of the observations and the timely public release of the data to ESO member-states.

<sup>1</sup> This major difference between the two families of models has been triggered by a diverging interpretation of the observed LMC supergiants oxygen abundances. A general agreement between various sources (cf Luck et al. 1998, Hill et al. 1997) has found  $[O/Fe]_{LMC}=-0.2$  from F-K supergiants, but, as argued by several authors (Luck & Lambert 1992, Hill et al. 1997, Pagel & Tautvaišiene 1998), this value should not be taken as absolute, but in reference to stars of similar type in the SN, which also give  $[O/Fe]_{LMC}=-0.2$  to  $-0.3$  dex, so that one can safely assume that  $[O/Fe]_{LMC}=[O/Fe]_{SN}$  at present time.

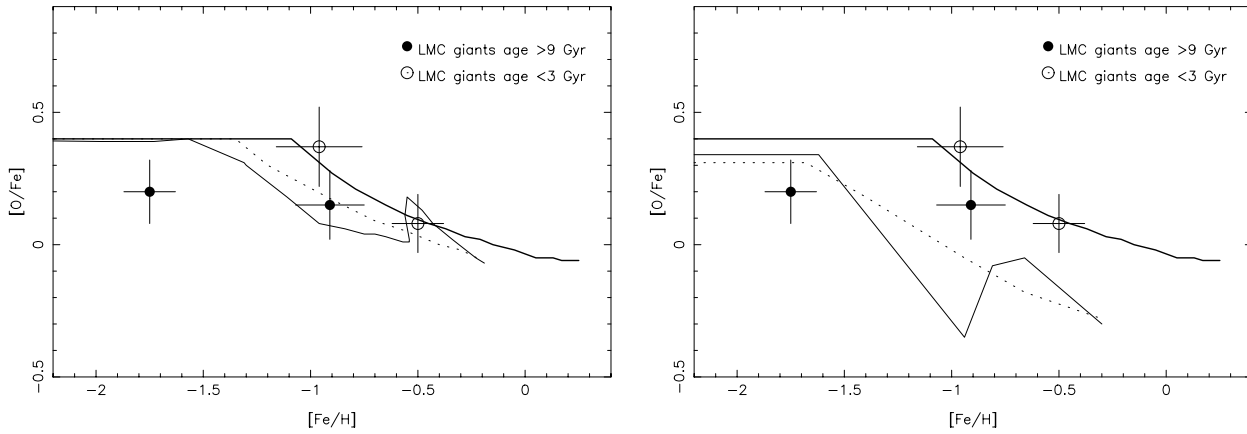


**Fig. 5.** Evolution of the oxygen over iron ratios with metallicity in the LMC. The mean oxygen abundance for the LMC clusters (this paper) are plotted together with LMC chemical evolution models using a bursting SFR (thin line) and a continuous SFR (dotted line) from: left panel Pagel & Tautvaišiene (1998) and right panel Tsujimoto et al. (1995). The thick line represents the behavior of  $[O/Fe]$  in our Galaxy (Pagel & Tautvaišiene 1995).

## References

- Alcaino G., Liller W., Alvarado F., Kravtsov V., Ipatov A., Samus N., Smirnov O., 1999, *A&AS* 135, 103
- Alonso A., Arribas S., Martínez-Roger C., 1999, *A&A* 140, 261
- Bertelli G., Bressan A., Chiosi C., Fagotto F., Nasi E., 1994, *A&AS* 106, 275
- Brocato E., Castellani V., Ferraro F. R., Piersimoni A. M., Testa V., 1996, *MNRAS* 282, 614
- Brocato E., Buonanno R., Castellani V., Walker A. R., 1989, *ApJS* 71, 25
- D’Odorico S., Cristiani S., Dekker H., Hill V., Kaufer A., Kim T., Primas F., 2000, in *SPIE 4005 Conf.* (in press)
- Dopita M. A., Vassiliadis E., Wood P. R., Meatheringham S. J., Harrington J. P., Bohlin R. C., Ford H. C., Stecher T. P., Maran S. P., 1997, *ApJ* 474, 188
- Edvardsson B., Andersen J., Gustafsson B., Lambert D.L., Nissen P.E., Tomkin J., 1993, *A&A* 275, 101
- Ferraro F. R., Fusi Pecci F., Testa V., Greggio L., Corsi C. E., Buonanno R., Terndrup D. M., Zinnecker H., 1995, *MNRAS* 272, 391
- Geisler D., Bica E., Dottori H., Claria J.J., Piatti A.E., Santos J.F.C.Jr, 1997, *AJ* 114, 1920
- Gustafsson B.E., Bell R.A., Eriksson K., Nordlund A., 1975, *A&A* 42, 407
- Hilker M., Richtler T., Gieren W., 1995, *A&A* 294, 648
- Hill V., Andrievsky S., Spite M., Spite F., 1995, *A&A* 293, 347
- Hill V., Barbuy B. and Spite, M., 1997, *A&A* 323, 461
- Johnson J. A., Bolte M., Stetson P. B., Hesser J. E., Somerville R. S., 1999, *ApJ* 527, 199
- Kraft R., Sneden C., Smith G.H., Shetrone M., Fulbright J., 1998 *AJ* 115, 1500
- Lloyd Evans, T., 1980, *MNRAS* 193, 87
- Luck R.E., Lambert D.L., 1992, *ApJS* 79, 303
- Luck R.E., Moffett T., Barnes T., Gieren W., 1998, *AJ* 115, 605
- Mateo M., Hodge P., Schommer R. A., 1986, *ApJ* 311, 113
- Olsen K. A. G., Hodge P. W., Mateo M., Olszewski E. W., Schommer R. A., Suntzeff N. B., Walker A. R., 1998, *MNRAS* 300, 665
- Olszewski E., Schommer R., Suntzeff N., Harris H., 1991, *AJ* 101, 5150 (O91)
- Pagal B. E., Tautvaišiene G., 1998, *MNRAS* 299, 535
- Pagal B. E., Tautvaišiene G., 1995, *MNRAS* 276, 505
- Plez B., private communication
- Schommer R., Olszewski E., Suntzeff N., Harris H., 1992, *AJ* 103, 447
- Shetrone M. D., 1996 *AJ* 112, 1517
- Tsujimoto T., Nomoto K., Yoshii Y., Hashimoto M., Yanagida S., Thielemann F.-K., 1995, *MNRAS* 277, 945
- Will J.-M., Bomans D.J., Tucholke H.-J., De Boer K.S., Grebel E.K., Richtler T., Seggewiss W., Vallenari A., 1995, *A&AS* 112, 367